Journal of Organometallic Chemistry, 394 (1990) 679–698
Elsevier Sequoia S.A., Lausanne
JOM 20801

A molecular orbital study of trinuclear platinum clusters *

D. Michael P. Mingos * and Tom Slee

Inorganic Chemistry Laboratory, University of Oxford, South Parks Road, Oxford OX1 3QR (U.K.)

(Received January 29th, 1990)

Abstract

Forty-four electron trinuclear *triangulo*-platinum clusters adopt a variety of geometrical conformations, unlike their forty-two electron homologues. Extended Hückel calculations are reported which throw light on electronic reasons for these different geometrical preferences, with particular emphasis on their bridging ligand dependence. It is shown that these geometrical preferences can be understood in terms of the frontier orbitals of mono-nuclear platinum fragments of the cluster.

Introduction

Transition metal complexes from Groups 6 to 9 obey the eighteen-electron rule closely, and the clusters of these elements obey the electron counting rules of the Polyhedral Skeletal Electron Pair Theory well [1]. The complexes and clusters of the late transition metals exhibit a greater flexibility in electron counts as a result of their large *d–p* promotion energies. The many sixteen and eighteen valence electron platinum complexes, of course, bear witness to this fact. Clusters of late transition metals are frequently characterised by fewer electrons than the clusters of the earlier transition elements [2].

There are several consequences of the valence flexibility of the late transition metals (platinum being of particular interest here). One is the different electron counts that can be accommodated by platinum clusters. Examples of trinuclear *triangulo*-platinum clusters have been synthesised with 42, 43, 44 and 46 valence electrons [3]. The 42-electron count is the most common, followed by 44; only one 46-electron and one 43-electron species have been reported with the triangle intact. Most of these trinuclear clusters contain a combination of PR_3, CO, SO_2 and isocyanide ($CNC_6H_4Me_2$-2,6) ligands. Although no 48-electron platinum triangles have been reported, Boag has reported a 48-electron palladium cluster, $[Pd_3(\eta_5\text{-}C_5Me_5)_3(\mu_3\text{-}CO)_2]^{2+}$ [4].

* Dedicated to Prof. Gordon Stone on his 65th birthday.

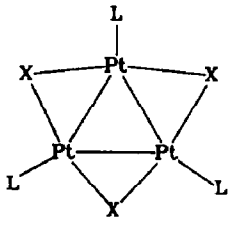

1

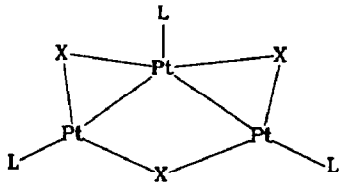

2

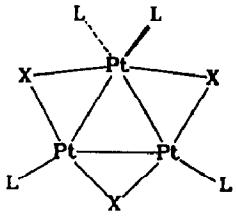

3

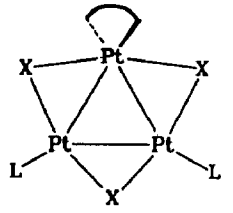

4

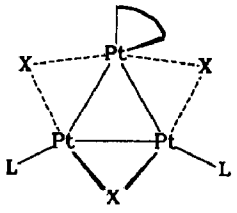

5

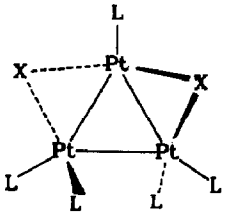

6

A second consequence is the structural variety exhibited by 44-electron trinuclear platinum clusters. While most 42-electron clusters exhibit D_{3h} or pseudo-D_{3h} geometries, as shown in **1**, the structures open to the 44-electron species include those shown as **2** to **10**.

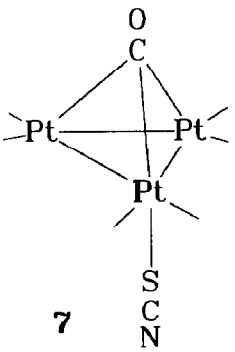

7

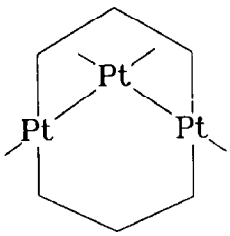

8

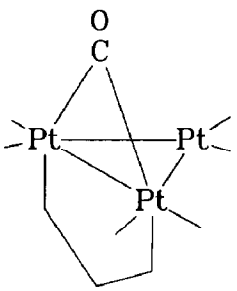

9

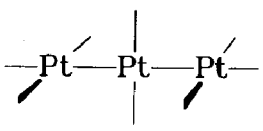

10

A third consequence can be seen in the addition and substitution chemistry of these Pt_3 species. Several reactions have been reported that maintain, in part or completely, the integrity of the Pt_3 unit [3]. The transformation between 42-electron and 44-electron *triangulo*-clusters can be effected by addition of terminal ligands [5], by substitution of a bidentate for a monodentate terminal ligand [6], by substitution of a bridging ligand [7], and by replacement of a bridging ligand by two terminal ligands [8]. The chemistry is dependent on the nature of the bridging ligand: for example, $Pt_3L_3(\mu\text{-}CO)_3$ (L = tertiary phosphine) reacts with isocyanide to give substitution products [9], $Pt_3L_3(\mu\text{-}SO_2)_3$ to give both substitution and addition products, which may involve replacing bridging ligands by terminal ligands and opening of the Pt_3 ring [8]. Introducing bridging isocyanide ligands into $Pt_3L_3(\mu\text{-}CO)_3$ makes the terminal phosphine labile, while no such effect is observed in the SO_2 analogue.

Valence flexibility also enables rearrangements of platinum clusters to take place. The 58-electron tetranuclear cluster $Pt_4(PR_3)_4(\mu\text{-}CO)_5$ adopts a butterfly geometry as shown in **11** [10,11], but NMR experiments [11] show that a rearrangement occurs which makes all four platinum atoms equivalent. It was suggested [11] that this rearrangement occurs through a tetrahedral intermediate geometry.

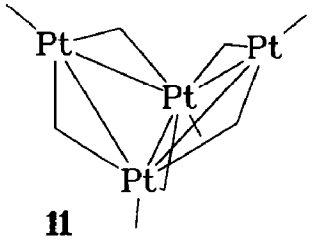

11

In this paper we seek to understand the structural diversity of 44-electron triplatinum clusters, and in particular the different structural behaviour exhibited by CO and SO_2-bridged species, using extend Hückel calculations.

Previous theoretical work on the electronic structure of platinum clusters has focused on the 42-electron triangles $Pt_3L_3X_3$, **1**, where the terminal ligand is denoted by L and the bridging ligand by X, a terminology we retain throughout. Some work has been done on extending electron-counting rules to larger platinum clusters, both through EHMO calculations for small clusters and by analogy with a radial bonding model originally developed for gold clusters, which can be applied to larger platinum clusters. A localised stereochemical model based on platinum's observed preferences in complexes has helped to explain some of the stereochemistry of platinum clusters. We review this work in the following section.

The only previous theoretical work focusing on reduced platinum triangles is that by Evans [12] who discussed electronic and structural features of clusters such as **7** and **9**. These clusters, made by Puddephatt and coworkers [13–16] have no μ_2-bridging ligands in the plane of the platinum triangle, the six in-plane sites being occupied by three bidentate phosphine ligands, bonding terminally. Extra ligands are then forced to take up positions out of the plane. Evans' study complements the present work, which focuses on the structural behaviour of 44-electron clusters with μ_2-bridging ligands.

Bonding in *triangulo*-triplatinum clusters

The observed electron counts of transition metal three-membered rings can be explained either in localised terms (treating each metal as if it were a complex centre) or in delocalised terms, in the spirit of the Polyhedral Skeletal Electron Pair Theory of cluster bonding. We first give the localised view.

A "complex" model of stereochemistry around platinum centres

Triangulo-clusters of, for example, the iron group can be described in terms of the eighteen-electron rule. $Os_3(CO)_{12}$ has 48 valence electrons, and adopts the structure **12** [17]. If we assume a single two-electron bond between each Os centre, then each osmium atom conforms to the eighteen-electron rule. In a similar manner, we can imagine 42-electron triplatinum clusters, **1**, to be comprised of three sixteen-electron platinum centres. If we decompose the cluster into a Pt_3L_3 fragment plus the three CO bridging ligands, then each PtL fragment has twelve electrons, so that the six electrons contributed by the bridging ligands must be responsible for metal–metal bonding through three-centre two-electron bonds.

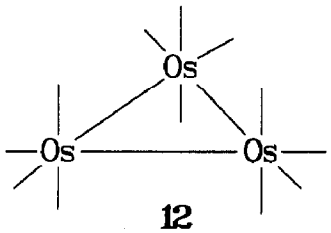

12

The addition of a terminal ligand, to give a structure such as **3**, leads to a 44-electron cluster [5] with one eighteen-electron and two sixteen-electron platinum centres. A recently reported 46-electron cluster, **9**, contains two eighteen-electron Pt centres [13].

Several aspects of the stereochemistry of these clusters can be understood from this point of view [3–6]. We take the known geometrical preferences of platinum complexes, and assume that each platinum centre will adopt a local geometry similar to one of these—in effect using a simple ball and stick model to rationalise the observed stereochemistry of trinuclear platinum clusters. Sixteen-electron platinum complexes are invariably square planar [1] (Fig. 1a) and this preference is reflected in the geometry around platinum in its trinuclear clusters. Figure 1b shows how a 42-electron triangle such as $Pt_3(CO)_3(PCy_3)_3$ [18] can been viewed as three T-shaped platinum centres [3], linked through the bridging ligands. The fourth point of the square would be the centre of the triangle in this model. The angles are all close to 90°. It is interesting that the metal–metal bonds do not appear to exert strong stereochemical influences.

Five-coordinate 18-electron Group 12 complexes are known with both trigonal bipyramidal and square pyramidal geometries [1], as shown in Fig. 1c, and fragments of both these are observed in the 44-electron clusters. Figure 1d shows the geometry of $Pt_3(\mu\text{-}CO)_3(PCy_3)_4$[5], in which the eighteen-electron platinum centre is based on a trigonal bipyramid, and Fig. 1e shows $Pt_3(\mu\text{-}SO)_2)_3(PCy_3)_3$(dppp) [6], in which the geometry around the eighteen-electron platinum centre is close to that

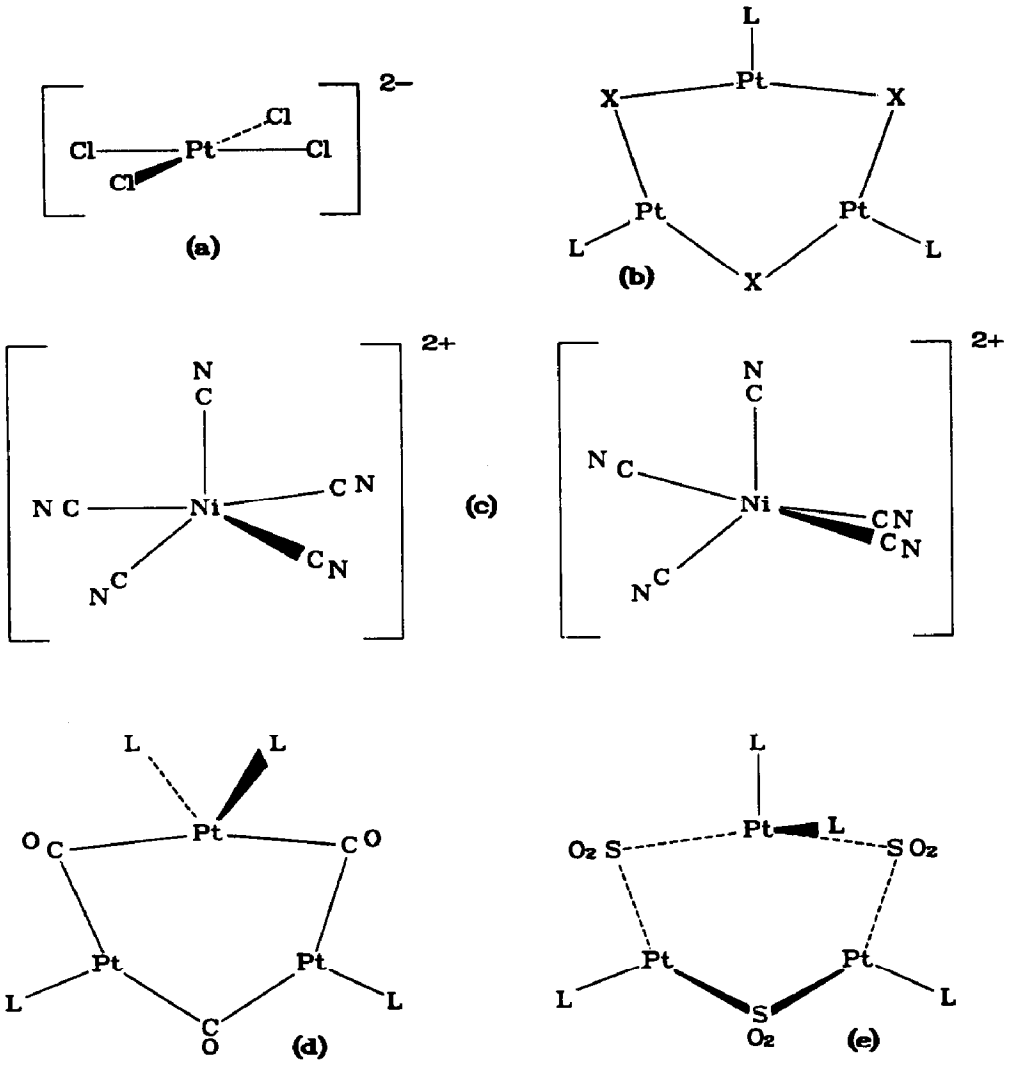

Fig. 1. Geometries around Group 12 centres in complexes and clusters. (a) A sixteen-electron square planar platinum complex. (b) A forty-two-electron trinuclear platinum cluster composed of three T-shaped platinum centres. (c) Geometries around nickel five-coordinate complexes include trigonal bipyramids and square pyramids. (d) Forty-four-electron trinuclear platinum clusters exhibit geometries around platinum centres based on both the shapes shown in (c). (e) Geometry around eighteen-electron platinum centre is close to that of a square pyramid.

of a square pyramid. In each case, the missing vertex of the coordination polyhedron is located in the centre of the triangle.

A delocalised description of the bonding in $Pt_3X_3L_3$ 42-electron clusters

A delocalised description has been developed, largely on the basis of extended Hückel calculations, in papers by Lauher [19], Rives et al. [20], Evans and Mingos [21], Underwood et al. [22], Gilmour and Mingos [24], and Mealli [25]. Consider the fragment comprised of the three platinum atoms and the three terminal ligands of a 42-electron $Pt_3L_3X_3$ cluster. The terminal ligands, L, are most often tertiary phosphines. For convenience, we employ a local set of axes at each atom such that

the x axis points radially towards the centre of the triangle, with z perpendicular to the ring. The occupied orbitals of this fragment consist of a set of three PtL bonding orbitals and a band of fifteen orbitals of predominantly metal d character. The LUMO, only slightly above the d band in energy, is an a_1' orbital composed of inwardly hybridised s and p_x orbitals on each platinum. At significantly higher energy there is an e' pair: the bonding combination of p_y orbitals. Above this are

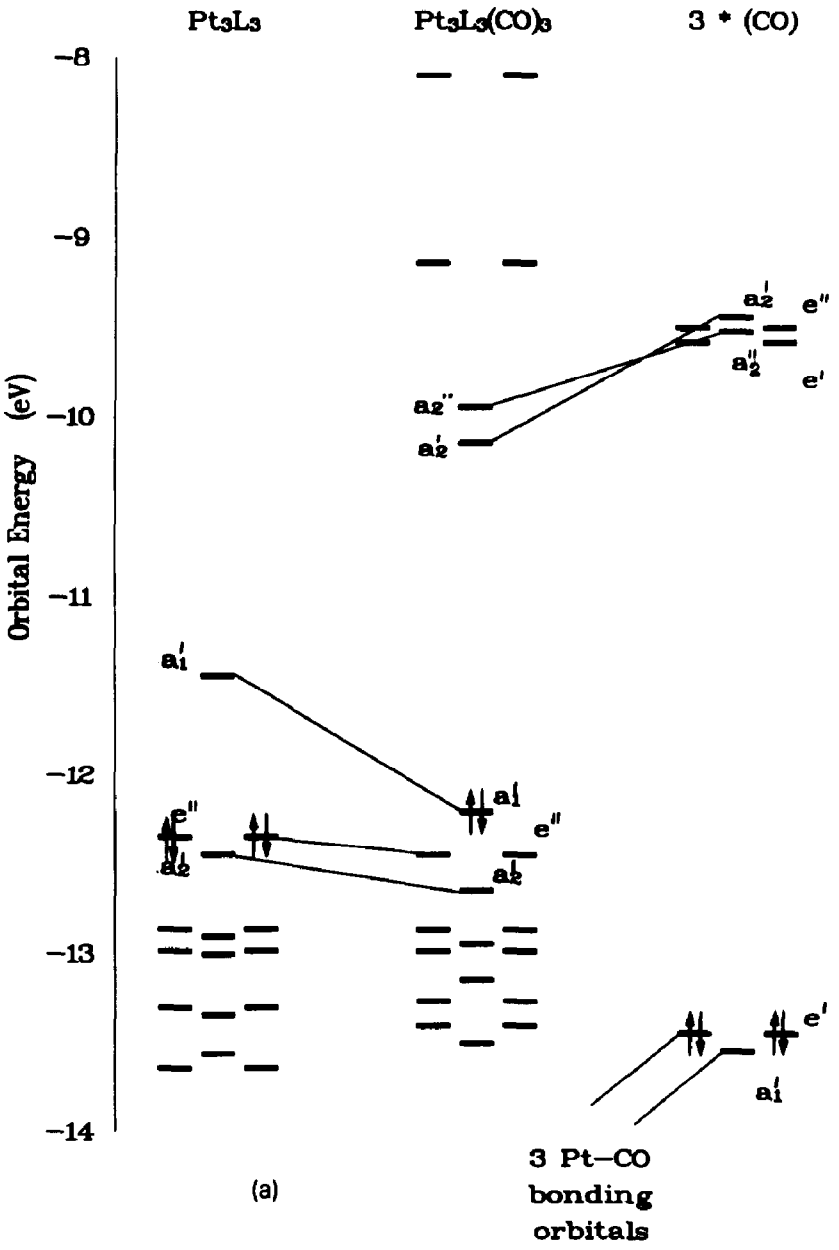

Fig. 2. (a) Orbital interaction diagram showing the formal combination of Pt_3L_3 with three CO bridging ligands to give $Pt_3L_3(CO)_3$. L is a modelled tertiary phosphine. The frontier orbitals of a_1', a_2' and a_2'' symmetry are of particular importance for our discussion, and are shown in (b). NLUMO indicates the Next to Lowest Unoccupied Molecular Orbital.

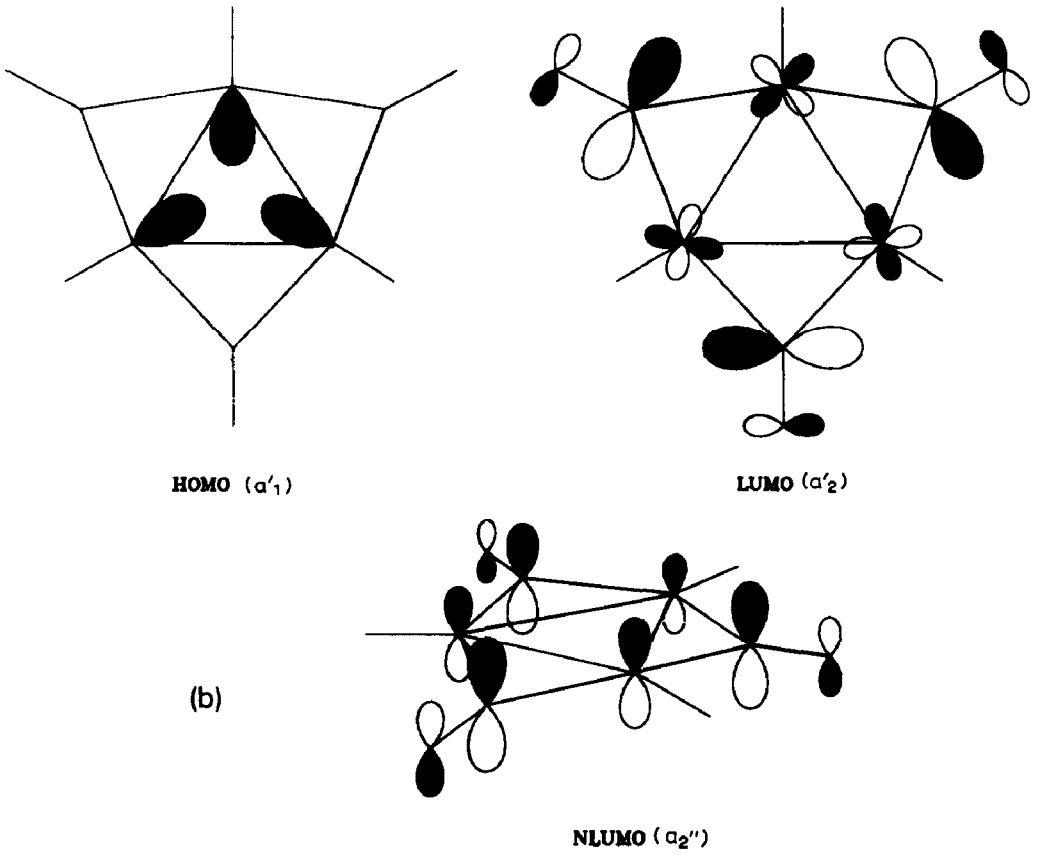

Fig. 2 (continued).

the bonding (a_2'') and antibonding (e'') combinations of the p_z orbitals, and at higher energy still is the a_2' antibonding p_y combination.

The a_1' and e' combinations of the lone-pair σ orbitals on the Lewis-base bridging ligands interact with orbitals of appropriate symmetry in both the occupied and vacant manifold of the Pt_3L_3 fragment. These are three-orbital interactions, and the result is to produce a bonding orbital below the *d*-band in energy, a non-bonding orbital localised mainly on the Pt_3L_3 fragment in the frontier orbital region at the top of the *d*-band, and an antibonding combination at higher energy. This is shown in Fig. 2a. The HOMO of the 42-electron cluster becomes the a_1' metal–metal bonding orbital. The composition of this orbital, which has significant metal *d*-character along with the bridging ligand and metal *s* contribution, can equivalently be described as a result of second-order mixing (polarisation) induced by the bridging ligands [25]. The two lowest unoccupied orbitals are the a_2'' bonding combination of metal p_z and CO π^* orbitals, and an a_2' orbital, which can be thought of as a bonding combination of in-plane CO π^* orbitals with the a_2' antibonding combination of metal p_y orbitals, although there is also metal *d*-orbital participation in this orbital. These orbitals, which are important for our discussion, are shown in Fig. 2b.

The relative energies of these unoccupied orbitals depend on the nature of the bridging and terminal ligands [22]. First-order perturbation theory tells us that both

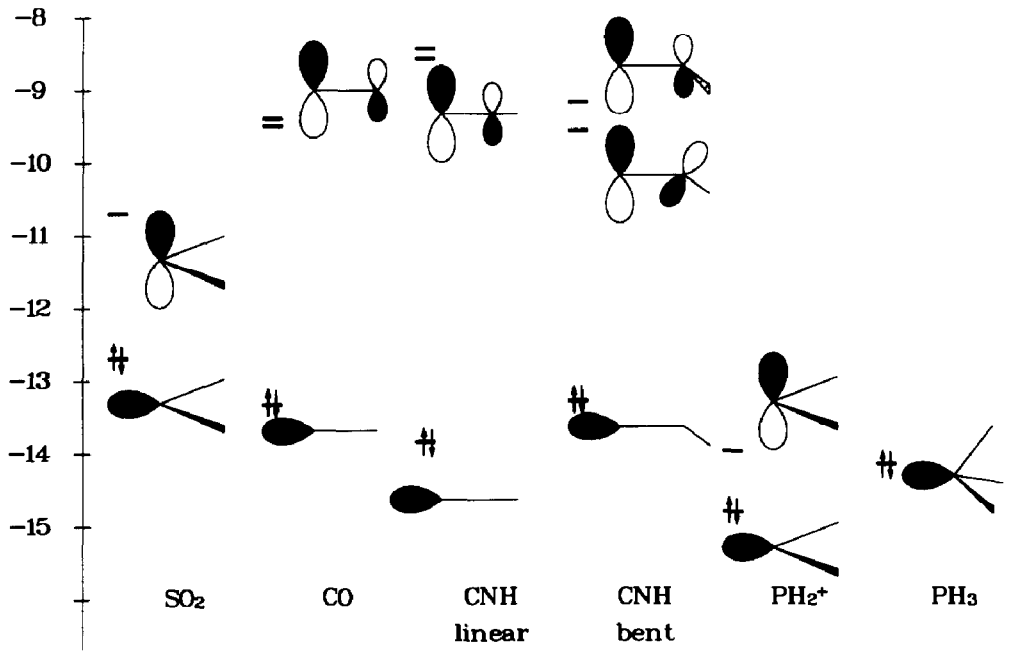

Fig. 3. Frontier orbitals for the ligands of interest in this paper; CNH, CO, SO_2, PH_2, and PH_3.

a_2'' and a_2' orbitals are stabilised by bridging ligands that have low-energy orbitals of appropriate symmetry. Figure 3 shows the frontier orbitals of models of the ligands of interest for this study: CNH, CO, SO_2, and PH_2, and it can be seen that at one extreme PH_2 will stabilise the a_2' orbital and produce a large gap above the a_2' orbital, whereas CO will have a large gap above the a_1' orbital. The energy levels of the frontier orbitals of 42-electron $Pt_3L_3X_3$ clusters with X = CO, PH_2, SO_2, and CNH are shown in Fig. 4.

Figures 2 and 4 suggest that there are two different ways of reducing the 42-electron cluster. The introduction of a halide anion, say, as one of the bridging ligands will lower the energy of the prevously unoccupied a_2' orbital, and populate it. The a_2'' orbital is perfectly suited for bringing up a Lewis base along the z axis and bonding it either to one of the platinum atoms or allowing it to "cap" the ring. The former process yields one eighteen-electron centre, while the latter adds two electrons to the cluster as a whole. Products of both these formal processes are known, and correspond to structures **4** to **6** and **7**, respectively. There is no obvious indication from this discussion as to whether substitution will lengthen all the Pt–Pt distances while keeping the triangle intact as in **1**, or whether it will open up the triangle as in **2**. Also, there is no obvious way of knowing whether addition will lead to **4**, **5**, **6**, or some other geometry.

In summary, previous work has shown that some structural aspects of the chemistry of trinuclear platinum clusters can be rationalised by the use of a ball-and-stick "complex" model, while the dependence of favoured electron count on bridging ligand can be explained from a delocalised viewpoint.

44-electron $Pt_3X_3L_3$ clusters

As described above, calculations on 42-electron clusters have shown that the low-lying vacant a_2' orbital is stabilised by π-acids. In many 44-electron $Pt_3X_3L_3$

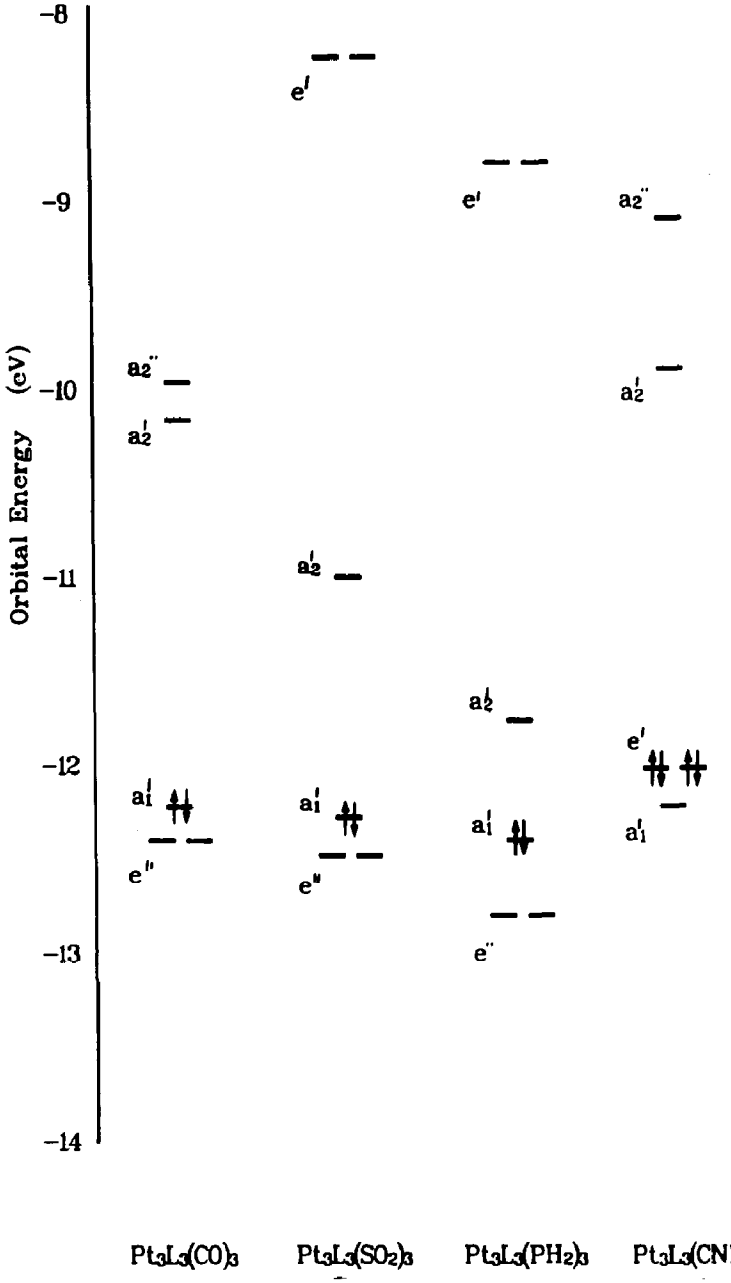

Fig. 4. Frontier orbital energies of forty-two electron *triangulo*-platinum clusters with different bridging ligands.

clusters this orbital, which is Pt–Pt antibonding, is occupied. Pt–Pt distances are thus generally longer in 44-electron clusters of this type [22].

In the present study, in which Pt–Pt lengths are fixed at 2.7 Å, the overlap populations were used to gauge the relative strengths of the metal-metal bonds. Figure 5 summarises the overlap populations for a variety of bridging ligand combinations. It can be seen that the Pt–Pt overlap populations are all significantly smaller for the 44-electron clusters than for the 42-electron clusters, as expected.

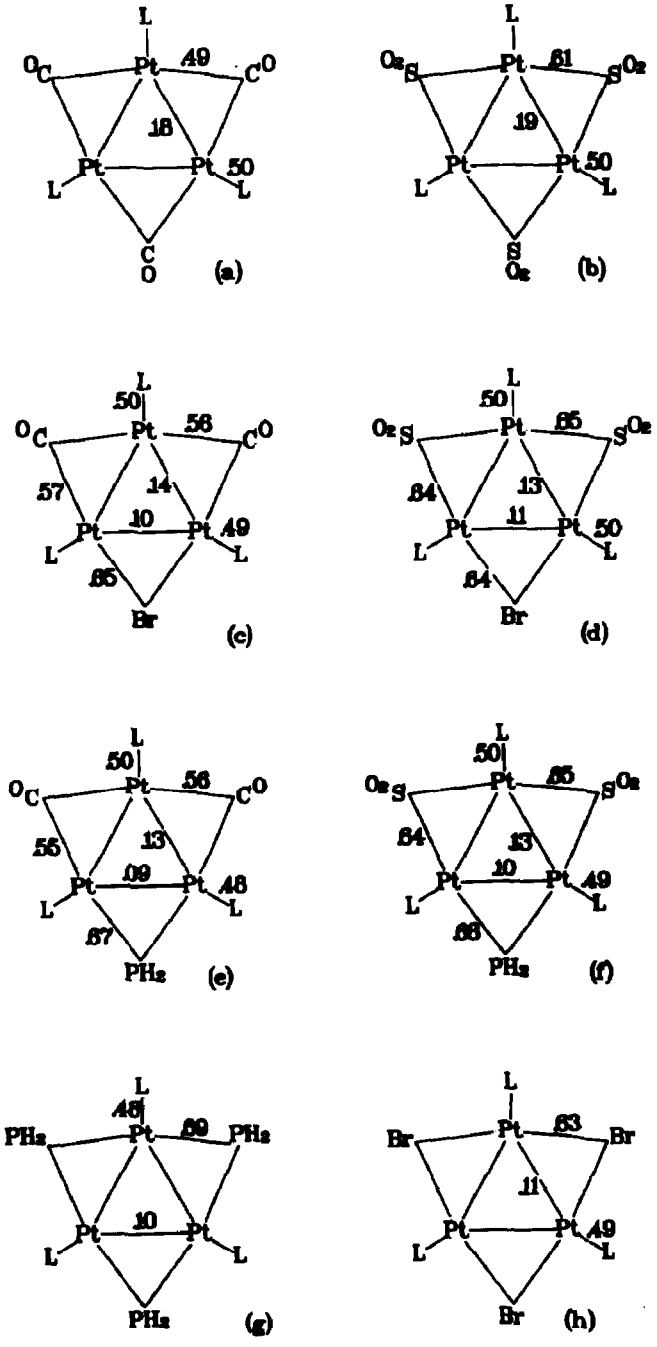

Fig. 5. Reduced overlap populations for a variety of six-ligand forty-four-electron trinuclear platinum clusters.

Further, the Pt–Pt edge bridged by the four-electron ligand (Br^-, PH_2^-) has a significantly lower overlap population than the edges bridged by two-electron donors (CO, SO_2).

A structural analysis on $[Pt_3(\mu\text{-}Br)(\mu\text{-}SO_2)_2(PCy_3)_3]$ (Cy = cyclohexyl, C_6H_{11}) [7], has been completed, but unfortunately, due to crystallographic disorder, only an

average Pt–Pt bond length could be reported. The average Pt–Pt distance is 2.886 Å, 0.175 Å longer than the comparable distance in $[Pt_3(SO_2)_3(PCy_3)_3]$ [7]. In the absence of crystallographic disorder one would anticipate that the metal-metal bond bridged by Br would be longer. The NMR coupling constant data on such compounds supports this proposal.

In the related 44-electron cluster $Pt_3(\mu\text{-}PPh_2)_3Ph(PPh_3)_2$ the edge bridged by PPh_2 is 3.63 Å, 0.845 Å longer than the other edges, as in **2** [23]. Extended Hückel calculations on $[Pt_3(\mu\text{-}PH_2)_3L_3]^+$, where L is a modelled tertiary phosphine ligand lone pair, as well as previous EHMO calculations [22,24,25], do not show the open triangle to be more stable than the triangular structure at this level of accuracy. There are, however, incipient signs of ring-opening in this structure. The PR_2 ligand has a pronounced weakening effect on the Pt–Pt overlap population. Further, comparison of the total energies show that the energy increase on opening the triangle is 7 kcal/mol less for the phosphide-bridged cluster than for the bromide-bridged cluster.

44-electron $Pt_3X_3L_4$ clusters

A crystal structure of $Pt_3(\mu\text{-}CO)_3(PCy_3)_4$ shows it to have the C_{2v} structure **3** [5], with one eighteen-electron platinum and two sixteen-electron centres. This molecule can be formally constructed from $Pt_3(\mu\text{-}CO)_3(PR_3)_3$ by replacing PtL with PtL_2. We look here at the changes this formal substitution produces in the cluster.

The frontier orbitals of PtL, and PtL_2 as a function of bending angle are shown in Fig. 6. The radial *sp* hybrid that contributes to the a_1' HOMO of $Pt_3(\mu\text{-}CO)_3L_3$ is raised in energy when the extra ligand is introduced, while the *p* orbital, which contributes to the a_2' LUMO, is unchanged. The PtL_2 HOMO, a *p-d* hybrid

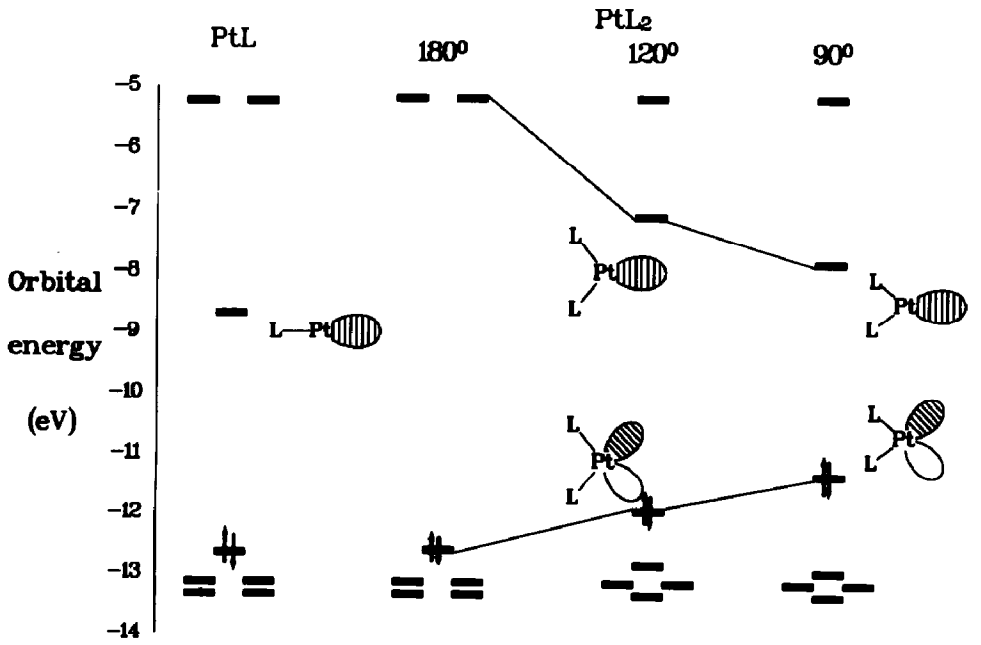

Fig. 6. Frontier orbitals of PtL and PtL_2 as a function of bending angle.

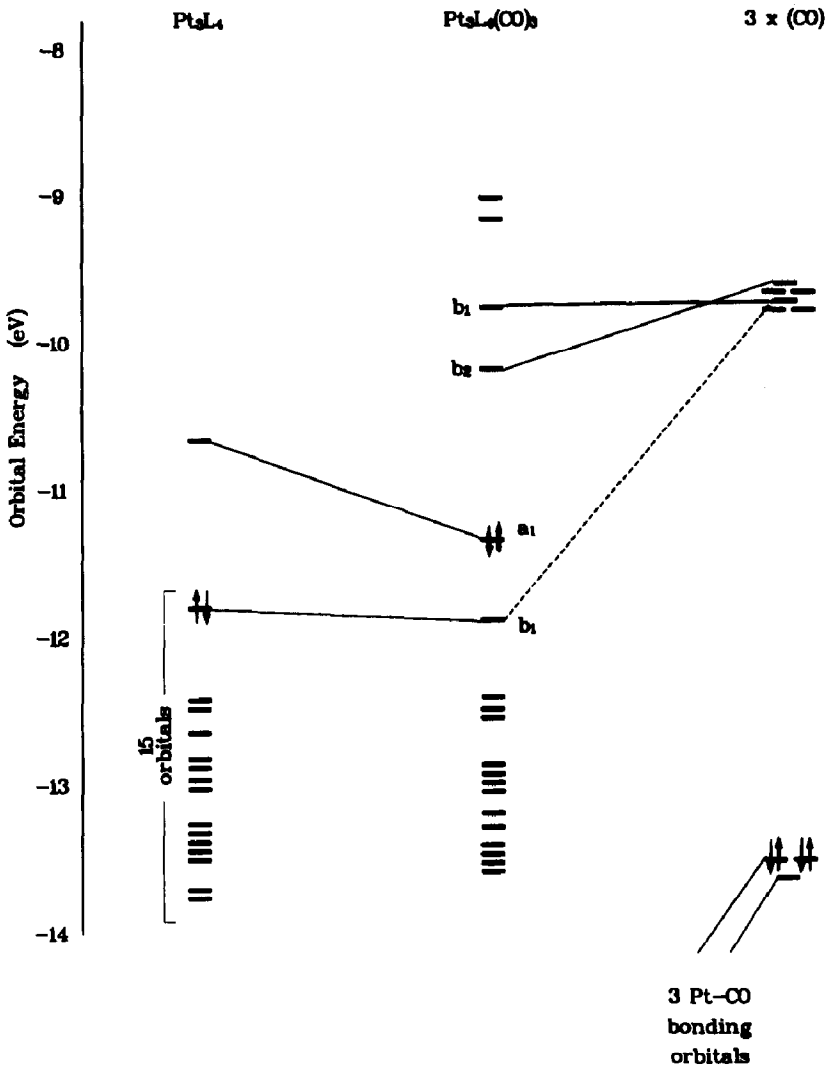

Fig. 7. Orbital interaction diagram showing the formal combination of Pt_3L_4 and three bridging CO ligands to give C_{2v} $Pt_3(CO)_3L_4$, where L is a modelled tertiary phosphine. The frontier orbitals should be compared to those of the forty-two electron cluster in Fig. 2.

coplanar with the PtL_2 nuclei, is raised in energy as the angle is decreased, while the energy of the *s-p* hybrid LUMO is lowered.

Figure 7 shows the electronic structure of $Pt_3(\mu\text{-}CO)_3L_4$, constructed from the Pt_3L_4 fragment and the bridging ligands. This figure should be compared to its 42-electron analogue (Fig. 2). The calculation was carried out for an L–Pt–L angle of 120°, close to the experimental angle of 126° [5]. The differences between the electronic structure of the seven- and six-ligand species can be understood in terms of the differences between the PtL and PtL_2 fragments. The cluster HOMO derived from inward-pointing *s-p* hybrids, is raised in energy by about 1.0 eV—almost exactly the same as the PtL_2 fragment component—while the energy of the LUMO remains the same. The frontier orbital gap is thus reduced, but remains greater than 1.0 eV. The HOMO of the PtL_2 fragment is closely related to the b_1 Pt_3L_4 fragment

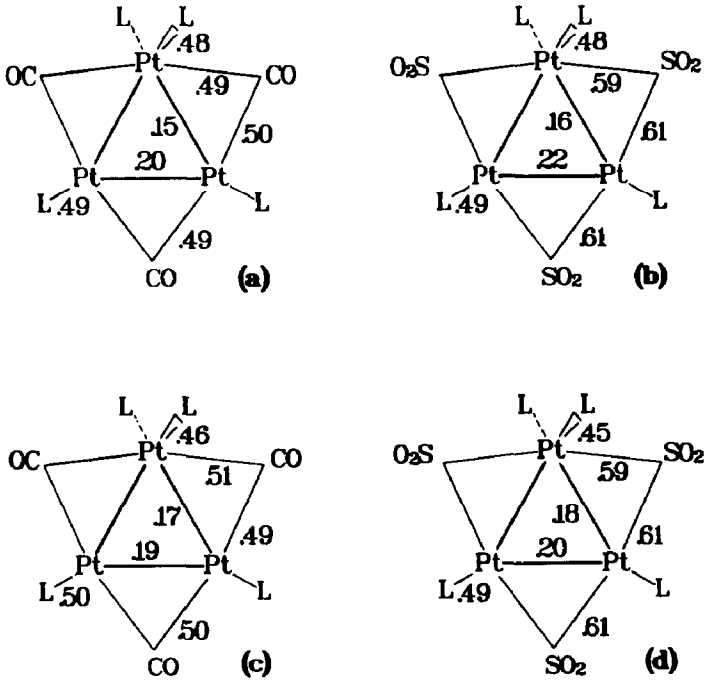

Fig. 8. Reduced overlap populations of seven-ligand, forty-four-electron trinuclear platinum clusters, for various combinations of bridging ligands.

HOMO. This interacts with the π^* orbitals of the bridging CO fragments and so is lowered slightly in energy, but is still the next highest orbital in energy to the HOMO of the cluster; it becomes important in the discussion below.

Reduced overlap populations, shown in Fig. 8, suggest that the bonds to PtL_2 will be longer than the LPt–PtL bond, and the crystal structure shows that this is indeed the case [5], the PtL_2–PtL bonds being 2.725 Å, compared to the LPt–PtL length of 2.675 Å. The overlap populations also suggest, however, that the LPt–PtL bond will be shorter than the metal–metal separation in the 42-electron analogue, while crystal structures show that the lengths are, in fact, very similar [5,18], the latter being 2.654 Å. Further, the overlap populations show that the bridging ligand is slightly more strongly bound to the PtL_2 moiety than the PtL. This is also reflected in the observed bond lengths, which show the L_2Pt–CO distance to be 0.03 Å shorter than the LPt–CO distance [5]. It should be pointed out that the "a_2''" orbital (b_1 in C_{2v} symmetry) is not occupied in this case, and so we would not expect the general expansion of the Pt_3 triangle predicted for the six-ligand case [22]: the electronic structure of the ring is altered in a quantitative manner, but remains qualitatively the same.

The high-lying occupied b_1 orbital of $Pt_3L_4(CO)_3$, descended from the HOMO of the PtL_2 fragment, makes the PtL_2 platinum centre nucleophilic in nature. This has stereochemical consequences in the 56-electron mixed cluster $[Pt_3Au(\mu_2\text{-}CO)_3(PPh_3)_5]^+$ [26]. This cluster, **13**, can be viewed as a 44-electron $Pt_3L_4(CO)_3$ cluster capped by an electrophilic $[AuPPh_3]^+$ fragment, with stereochemistry determined primarily by the b_1 high-lying orbital of the platinum triangle. The gold atom is 2.700 Å from the PtL_2 platinum, and 2.906 Å from the other platinum

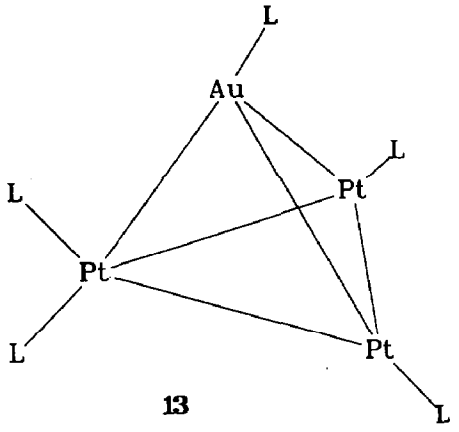

13

centres; it is closer to the sterically more crowded PtL_2 centre. The orientation of the $[AuPPh_3]^+$ fragment is such that its *s-p* hybrid LUMO is pointing towards the highly coordinated platinum atom.

By reacting $Pt_3(\mu\text{-}CO)_3(PCy_3)_3$ with dppp, a $Pt_3X_3L_4$ cluster is formed [6] in which the dppp backbone "ties together" the terminal ligands, reducing the P–Pt–P angle to close to 90°. No crystal structure has been reported for this cluster, but NMR data suggests that it adopts the C_{2v} structure **4**. How does this "tying together" influence the electronic structure of the cluster?

We consider first the PtL_2 fragment. Figure 6 above shows that decreasing the L–Pt–L angle stabilises the radial sp hybrid by over 0.5 eV. At 120° the cluster HOMO is the a_1 analogue of the a_1' 42-electron species HOMO and is raised in energy along with the PtL_2 *sp* hybrid that is a major contributor to it.

As the L–Pt–L angle is closed to 90° the energy of the PtL_2 HOMO (see Fig. 6), and the cluster b_1 orbital it corresponds to (see Fig. 9), is raised, while the energy of the PtL_2 LUMO is lowered. This produces a crossing of the cluster frontier orbitals, as shown in Fig. 9. The energy of the resulting HOMO in the two cases is, however, essentially unchanged. The LUMO is unchanged in both character and energy, so the HOMO–LUMO gap is overall unchanged by the "tying together" of the terminal ligands.

The SO_2-bridged analogue of the $Pt_3(\mu\text{-}CO)_3L_4$ species is not known. We look at the electronic structure such a species would have if it adopted the C_{2v} structure **4**, in order to study the differences between CO and SO_2 as a bridging ligand. Also, a chelated cluster with four terminal ligands and three bridging SO_2 ligands is known. $Pt_3(\mu\text{-}SO_2)_3(PCy_3)_2(dppp)$ adopts a geometry close to that of **5**, substantially distorted from planarity, in marked contrast to the CO analogue [6]. It there an electronic reason for this difference?

Figure 10 shows an interaction diagram for the formal combination of Pt_3L_4 and the three SO_2 ligands, at L–Pt–L angles of 120° and 90° (and should be compared to the analogous Figure 9). The LUMO of the cluster in both cases is the b_2 analogue of the a_2' 42-electron species LUMO. It is lower in energy than in the CO-bridged species. The two occupied orbitals highest in energy are very similar to the CO-bridged case, being derived from the PtL_2 frontier orbitals. There is,

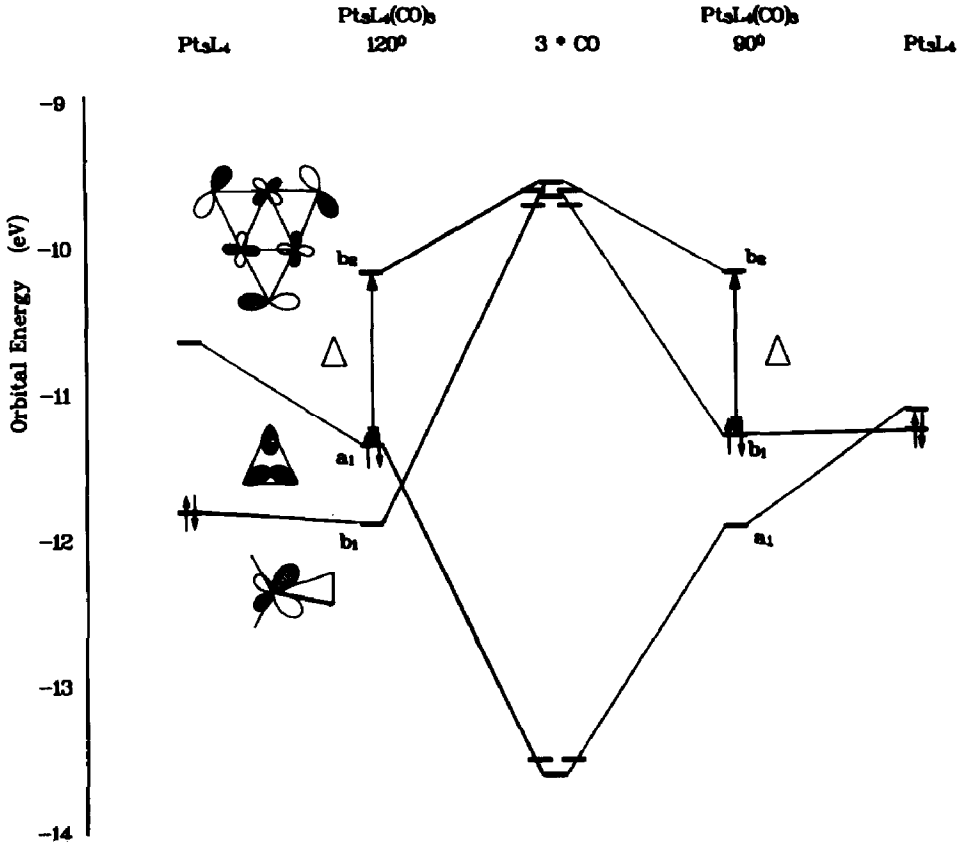

Fig. 9. Orbital interaction diagram showing the changes induced in the frontier orbitals by the "tying together" of two phosphine ligands. This tying together mimics the replacement of two phosphine ligands by one chelated phosphine ligand. The frontier orbital gap remains constant, even though there is an orbital crossing in the occupied manifold which changes the nature of the HOMO. The principal nodal characteristics of the frontier orbitals are shown.

however, no analogue to the interaction with CO π^* orbitals, and so the HOMO in the chelated SO_2-bridged cluster is somewhat higher in energy than the CO analogue. The net result is a very small frontier orbital gap in the SO_2-bridged species, and particularly in the chelated case. The chelated cluster distorts to become non-planar (structure **5**) and opens up a HOMO–LUMO gap of 1.3 eV. It is possible that the $Pt_3(PR_3)_4(SO_2)_3$ would also distort in this manner.

The small HOMO–LUMO gap of C_{2v} $Pt_3L_4(SO_2)_3$ shown in Fig. 10 is a result of the high-lying occupied b_1 orbital descended from the HOMO of the PtL_2 fragment. The LUMO of the PtL_2 moiety is the radial *s-p* hybrid. These two orbitals are the key to the opening up of a significant HOMO–LUMO gap in the bent structure **5**. If the PtL_2 part of the Pt_3L_4 fragment is bent out of the plane, these two frontier orbitals become of the same symmetry and mix. Crucially, the fragment HOMO becomes involved in metal–metal bonding and so is lowered in energy, as shown in the interaction diagram (Fig. 11). The Pt_3L_4 LUMO is an *spd* hybrid pointing away from the out-of-plane PtL bond, as shown in Fig. 12.

The out-of-plane bending of the PtL_2 moiety destroys one plane of symmetry of the molecule, reducing the symmetry to C_s. The SO_2 ligands also move out of the

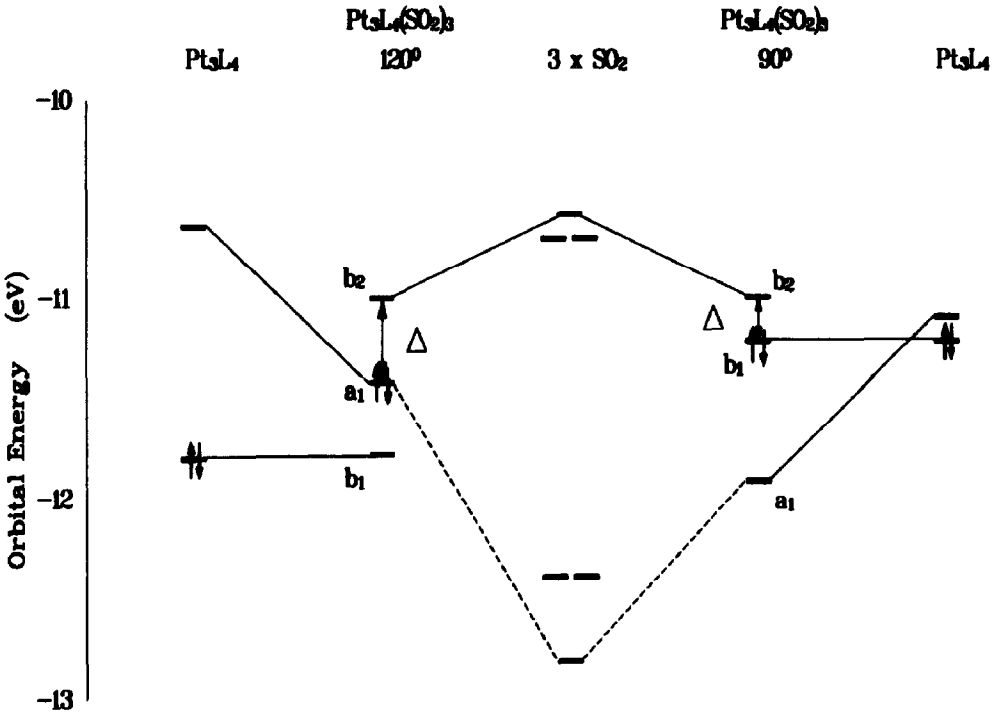

Fig. 10. Orbital interaction diagram showing the effect of "tying together" the phosphine ligands in a forty-four-electron SO_2-bridged cluster. The frontier orbitals are similar in composition to those of the CO-bridged compound shown in Fig. 9. The frontier orbital gap is small compared with the forty-two electron case, and is particularly small in the case of the chelated cluster. The cluster distorts to become non-planar.

plane of the platinum triangle to take advantage of the altered frontier orbitals of the Pt_3L_4 fragment. Two SO_2 ligands take up positions on the opposite side of the plane to the out-of-plane PtL bond, so as to interact more strongly with the LUMO

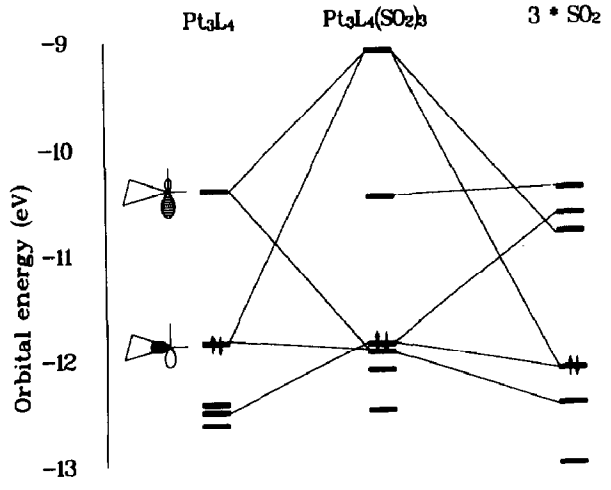

Fig. 11. An interaction diagram for the C_s geometry of $Pt_3L_4(SO_2)_3$. Comparison with Fig. 10 shows how the HOMO-LUMO gap is opened up by lowering of the HOMO energy.

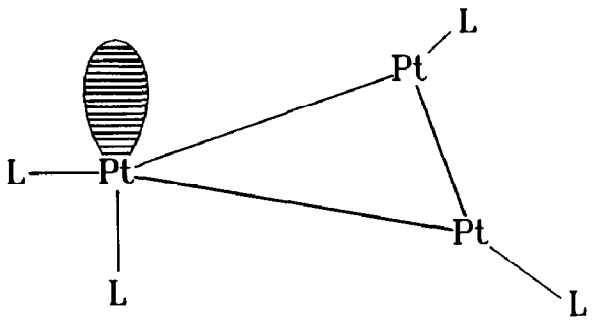

Fig. 12. The *spd* hybrid composition of the frontier orbital of the C_s Pt_3L_4 fragment. Such orbitals play an important role in determining the stereochemistry of some reduced platinum clusters.

of the Pt_3L_4 fragment. The third SO_2 fragment is on the same side of the platinum triangle plane as the PtL bond, so that each of the three-coordinate platinum atoms maintain a T-shaped local geometry [3].

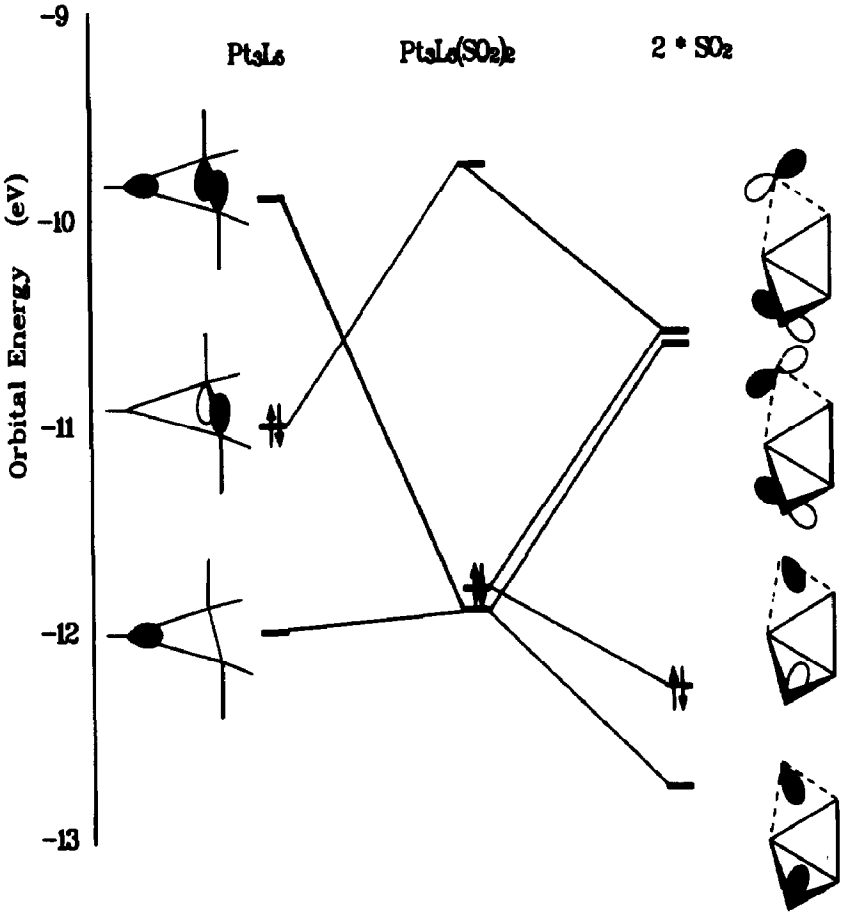

Fig. 13. A frontier interaction diagram for $Pt_3L_5(SO_2)_2$, showing the predominantly *p-d* hybrid composition of the Pt_3L_5 fragment and the way in which they are set up to interact with the *trans* arrangement of the two SO_2 bridging ligands.

A 44-electron $Pt_3X_2L_5$ cluster

The role of frontier orbitals such as the spd hybrid LUMO of the Pt_3L_4 fragment was emphasised by Evans [12] in his study of reduced platinum triangles. This type of orbital also accounts for the structure adopted by $[Pt_3(CNR)_2(PCy_3)_3(SO_2)_2]$, 6 above [8]. The three terminal tertiary phosphine ligands are coplanar with the platinum triangle, while two terminal isocyanide ligands adopt positions out of the plane of the platinum triangle, on opposite sides. The SO_2 ligands then bond trans to the neighbouring isocyanide ligand, so as to better interact with the hybrid frontier orbitals of the Pt_3L_5 fragment. A frontier orbital interaction diagram of this cluster is shown in Figure 13, which shows how the *spd* hybrid orbitals are the predominant contributors to the frontier orbitals of the Pt_3L_5 fragment, and how they are set up to interact with trans bridging ligands. These interactions and their stereochemical consequences are similar to those described by Evans [12].

Conclusions

Extended Hückel calculations combined with orbital interaction techniques have proved in the past to be very powerful methods for understanding conformational variations in clusters. In this paper these methods have been applied to the conformational options open to 44-electron platinum clusters. It has been shown that the extended Hückel approximation is sufficient to reproduce the trends of interest, and that the origins of the conformational preferences include electronic

Table 1

Parameters used in extended Hückel calculations

Atom	Orbital	H_{ii} (eV)	ζ_1	ζ_2	C_1	C_2
H	1*s*	−13.60	1.300			
C	2*s*	−21.40	1.625			
C	2*p*	−11.40	1.625			
N	2*s*	−26.00	1.950			
N	2*p*	−13.40	1.950			
O	2*s*	−32.30	2.275			
O	2*p*	−14.80	2.275			
S	3*s*	−20.00	1.817			
S	3*p*	−13.30	1.817			
P	3*s*	−18.60	1.600			
P	3*p*	−14.00	1.600			
Pt	5*d*	−13.16	6.010	2.696	0.6332	0.5512
Pt	6*s*	−10.75	2.550			
Pt	6*p*	−5.27	2.550			
Br	4*s*	−22.07	2.588			
Br	4*s*	−13.10	2.131			
'L'	(1*s*)	−14.2	1.300			

factors, even in these sterically crowded species. These factors can be traced back to the simple frontier orbitals of mononuclear platinum centres.

Computational methods

We employed extended Hückel calculations [27] without charge iteration. Terminal tertiary phosphine ligands were simulated by a hydrogen 1*s* orbital at −14.2 eV (the energy of the PH_3 lone pair). Parameters employed are shown in Table 1, and are essentially those used by Underwood et al. [22]. Pt–Pt distances were fixed at 2.7 Å, Pt–L at 1.7 Å, C–O at 1.2 Å, S–O at 1.45 Å, and Pt–μ-CO and Pt–μ-SO_2 were fixed at 2.0 Å.

Acknowledgements

We thank the SERC for funding this project, and thank Mr. Lin Zhenyang and Mr. Michael. J. Watson for helpful discussions.

References

1 N.N. Greenwood and A. Earnshaw, Chemistry of the Elements, Pergamon, Press, Oxford, 1984.
2 F.R. Hartley, in G. Wilkinson, F.G.A. Stone and E.W. Abel, (Eds.), Comprehensive Organometallic Chemistry, Pergamon Press, Oxford, 1982, Vol. 6, p. 471.
3 D.M.P. Mingos, Transition Met. Chem., 10 (1985) 441.
4 N.M. Boag, D. Boucher, J.A. Davies, R.W. Miller, A.A. Pinkerton and R. Syed, Organometallics, 7 (1988) 791.
5 A. Albinati, G. Carturan and A. Musco, Inorg. Chim. Acta, 16 (1979) L3.
6 M.F. Hallam, N.D. Howells, D.M.P. Mingos and R.W.M. Wardle, J. Chem. Soc., Dalton Trans., (1985) 845.
7 S.G. Bott, M.F. Hallam, O.J. Ezomo, D.M.P. Mingos and I.D. Williams, J. Chem. Soc., Dalton Trans., (1988) 1461.
8 D.M.P. Mingos, I.D. Williams and M.J. Watson, J. Chem. Soc., Dalton Trans., (1988) 1509.
9 C.E. Briant, D.I. Gilmour, D.M.P. Mingos and R.W.M. Wardle, J. Chem. Soc., Dalton Trans., (1985) 1693.
10 R.G. Vranka, L.F. Dahl, P. Chini and J. Chatt, J. Am. Chem. Soc., 91 (1969) 1574.
11 A. Moor, P.S. Pregosin, L.M. Venanzi and A.J. Welch, Inorg. Chim. Acta, 84 (1984) 103.
12 D.G. Evans, J. Organomet. Chem., 352 (1988) 397.
13 S.S.M. Ling, N. Hadj-Bagheri, L. Manojlovic-Muir, K.W. Muir and R.J. Puddephatt, Inorg. Chem., 26 (1987) 231.
14 B.R. Lloyd, A. Bradford and R.J. Puddephatt, Organometallics, 6 (1987) 424.
15 G. Ferguson, B.R. Lloyd, L. Manojlovic-Muir, K.W. Muir and R.J. Puddephatt, Inorg. Chem., 25 (1986) 4190.
16 G. Ferguson, B.R. Lloyd and R.J. Puddephatt, Organometallics, 5 (1986) 344.
17 K. Wade, in B.F.G. Johnson (Ed.), Transition Metal Clusters, J. Wiley, Chichester, 1980.
18 A. Albinati, Inorg. Chim. Acta, 22 (1977) L31.
19 J.W. Lauher, J. Am. Chem. Soc., 100 (1978) 5305.
20 A.B. Rives, Y. Xiao-Zeng and R.F. Fenske, Inorg. Chem., 21 (1982) 2286.
21 D.G. Evans and D.M.P. Mingos, J. Organomet. Chem., 240 (1982) 321.
22 D.J. Underwood, R. Hoffmann, K. Tatsumi, A. Nakamura and Y. Yamamoto, J. Am. Chem. Soc., 107 (1985) 5968.
23 N.J. Taylor, P.C. Cheih and A.J. Carty, J. Chem. Soc., Chem. Commun., (1975) 448.
24 D.I. Gilmour and D.M.P. Mingos, J. Organomet. Chem., 302 (1986) 127.

25 C. Mealli, J. Am. Chem. Soc., 107 (1985) 2245.
26 J.J. Bour,, R.P.F. Kanters, P.P.J. Schebos, W. Bos, W.P. Bosman, H. Behm, P.T. Beurskens and J.J. Steggerda, J. Organomet. Chem., 329 (1987) 405.
27 R. Hoffmann and W.N. Lipscomb, J. Chem. Phys., 36 (1962) 2179; R. Hoffmann and W.N. Lipscomb, J. Chem. Phys., 37 (1963) 2872; R. Hoffmann, J. Chem. Phys., 39 (1965) 1397.